Fault Diagnosis and Prognosis of a Brushless DC motor using a Model-based Approach

Joaquim Blesa, Joseba Quevedo, Vicenç Puig, Fatiha Nejjari, Raúl Zaragoza and Alejandro Rolán

Supervision, Safety and Automatic Control Research Center (CS2AC)
Universitat Politècnica de Catalunya (UPC),Campus de Terrassa,
Gaia Building, Rambla Sant Nebridi, 22
08222 Terrassa, Barcelona

{joaquim.blesa, joseba.quevedo, vicenc.puig, fatiha.nejjari, alejandro.rolan}@upc.edu

raul.zaragoza@estudiant.upc.edu

ABSTRACT

This paper proposes a model-based fault diagnosis and prognosis approach applied to brushless DC motors (BLDC). The objective is an early detection of mechanical and electrical faults in BLDC motors operating under a variety of operating conditions. The proposed model-based method is based on the evaluation of a set of residuals that are computed taking into account analytical redundancy relations. Fault diagnosis consist of two steps: First, checking if at least one of the residuals is inconsistent with the normal operation of the system. And, second, evaluating the set of the residuals that are inconsistent to determine which fault is present in the system. Fault prognosis consists of the same two steps but instead of considering current inconsistencies evaluates drift deviations from nominal operation to predict futures residual inconsistencies and therefore predict future fault detections and diagnosis. A description of various kinds of mechanical and electrical faults that can occur in a BLDC motor is presented. The performance of the proposed method is illustrated through simulation experiments.

1. INTRODUCTION

In the last years, a growing industrial interest in fault diagnosis and more recently in fault prognosis is perceived in the research community. In the scientific literature, fault diagnosis is nowadays a quite mature field with well-established approaches (see as e.g. Blanke el al., 2006, Ding, 2008, Escobet et al., 2019). However, prognosis is still in a less mature stage where most of the approaches existing are quite ad-hoc to the application.

In this paper, the extension of the well-established model-based fault diagnosis approaches to deal with prognosis will be proposed. This idea has already been explored by several researchers (Roychoudhury et al., 2006; Yu et al., 2011). In fact, fault diagnosis methods for incipient faults are suitable to be extended for prognosis.

This paper proposes a model-based fault diagnosis and prognosis approach applied to brushless DC motors. The objective is an early detection of rotor and load faults in BLDC motors operating under a variety of operating conditions. This involves recognizing the rotor and fault signatures produced in BLDC motors, and estimating the severity of the fault. A description of various kinds of rotor and load faults that can occur in a BLDC motor is presented. The effects of various types of faults on the motor current or voltage, which represent an alternative to vibration-based diagnostics, are investigated and illustrated through simulation experiments.

The structure of the paper is the following: Section 2 presents the problem statement and an overview of the proposed solution. Section 3 presents the fault diagnosis and prognosis approach. Section 4 describes the case study based on a brushless DC motor including the model and the fault scenarios considered. Section 5 presents the results. Finally, Section 6 draws the main conclusions.

2. PROBLEM STATEMENT: MODEL-BASED DIAGNOSIS/PROGNOSIS

2.1. Problem statement

Given a model of the system and a set of output observed variables, y_k , and the set of inputs, u_k , consistency tests can be derived from an analytical redundancy relation

(ARR) by generating a computational residual in the following way (see Blanke et al., 2006):

$$r_i = \Psi_i\left(y_k, u_k\right) = 0, \tag{1}$$

where Ψ_i is called the residual ARR expression. The set of ARRs can be represented as

$$\mathcal{R} = \left\{ r_i = \Psi_i\left(y_k, u_k\right) = 0, i = 1, \cdots, n_r \right\}, \tag{2}$$

where n_r is the number of ARRs obtained after applying the structural analysis.

Let $\mathcal{F}$ be the set of faults that must be monitored.

In this paper, a model based approach using residuals obtained from the ARRs (2) that will be used for dealing with the fault diagnosis and prognosis problems is introduced in the following.

Problem 1. "*Fault diagnosis*". Fault diagnosis aims at detecting and identifying the fault that is affecting a system in a fault scenario given a sequence of values of the output observed variables, y_k, and the set of inputs, u_k, and the considered set of faults $\mathcal{F}$ and ARRs in (2).

That is, fault diagnosis is about detecting and isolating a fault that has already occurred in the system. On the other hand, fault prognosis is about anticipating the appearance of a fault in time. Thus, the second problem addressed in this paper is defined as follows.

Problem 2. "*Fault prognosis*". Fault prognosis aims at predicting the appearance of fault in the system in a given time horizon from the current time given a sequence of values of the output observed variables, y_k, and the set of inputs, u_k, and the considered set of faults $\mathcal{F}$ and ARRs in (2).

2.2. Overview of the proposed approach

The proposed approach is based on the following modules:

- residual generation via the ARRs (2). Using the sequence of values of the output observed variables, y_k, and the set of inputs, u_k, the ARRs will be evaluated using their mathematical expressions generating a set of residuals.
- residual analysis via two processes: every ARR will be evaluated against its corresponding detection threshold. If the threshold is violated, a fault is indicated. A further analysis is required matching the violated residuals against the fault signature matrix to discover the fault affecting the system among the set of considered faults $\mathcal{F}$. If the residual is not violated, the residual value in a time horizon is evaluated to detect some trend. If a significant trend is detected, it is projected towards the future to determine the time required for residual to violate its threshold. From this information, the fault prognosis algorithm will be able to predict the appearance of a fault in a given time horizon.

3. PROPOSED SOLUTION: FAULT DIAGNOSIS/PROGNOSIS USING ANALYTICAL REDUNDANCY RELATIONS

Using the set of computable ARR residuals (1), the fault detection module must check at each time instant whether or not the ARRs are consistent with the observations. Under ideal conditions, residuals are zero in the absence of faults and non-zero when a fault is present. However, modeling errors, disturbances and noise, in complex engineering systems are inevitable, and hence it appears the necessity of applying robust fault detection algorithms.

3.1. Residual generation

Taking into account bounded uncertainties, the residuals (1) can be rewritten as follows:

$$r_i = \Psi_i\left(y_k, u_k, \theta_k\right) \tag{3}$$

with: $\theta_k \in \Theta$, where Θ is the interval box $\Theta = \left\{ \theta \in \mathbb{R}^{n_\theta} \middle| \underline{\theta} \le \theta \le \overline{\theta} \right\}$, that includes all uncertainties (i.e. disturbances/model errors and measurement noise). Then, fault detection can be formulated as checking the consistency of (3) using a set-membership approach (Puig et al., 2013).

Definition 1. *"Consistency checking"*. Given the residuals described by (3) and a sequence of measured inputs u_k and outputs y_k of the real system at time *k*, they are consistent with measurements and uncertainty bounds if there exist a set of sequences $\theta_k \in \Theta$ that satisfies $r_i = 0$.

Thus, according to this definition, a residual consistency is equivalent to check if $0 \in \left[r_i(k)\right]$ where $\left[r_i(k)\right]$ is the interval that bounds the effect of uncertainty in the residual (3).

3.2. Residual analysis

Definition 2. *Fault detection*. Given a sequence of observed inputs u_k and outputs y_k of the real system, a fault is said to be detected at time *k* if there does not exist a set of uncertainty sequences $\theta_k \in \Theta$ to which the set of ARRs is consistent.

In case that $0 \in \left[r_i(k)\right]$, although a fault is detected, the evolution of the residual can be forecasted *h*-steps ahead using the Brown's Double Exponential Smoothing is used (S. Hansun, 2016) that is based on the following multi-step forecast formula

$$\hat{r}_i(t) = \alpha r_i(t) + (1-\alpha)\hat{r}_i(t-1)$$

$$\breve{r}_i(t) = \alpha r_i(t) + (1-\alpha)\breve{r}_i(t-1) \quad (4)$$

$$\hat{r}_i(k+h\,|\,k) = \left(2+\alpha\frac{h}{1-\alpha}\right)\hat{r}_i(k) - \left(1+\alpha\frac{h}{1-\alpha}\right)\breve{r}_i(k)$$

where h is the forecasting horizon and α the smoothing parameter. The parameter α is obtained from historical data using parameter estimation by means of the least squares algorithm using a moving horizon time window L.

The Remaining Useful Life (RUL) forecasted by the residual r_i based on the corresponding threshold given by the residual interval $[r_i(k)]$ can be determined as follows

$$RUL_i \in \mathbb{Z}_{\geq 0} \,|\, 0 \notin \left[\hat{r}_i(k+RUL_i\,|\,k)\right] \quad (5)$$

where $\hat{r}(k+RUL\,|\,k)$ is the RUL-step ahead forecast at time k of the corresponding predictive model (4).

3.3. Fault diagnosis

According to Definition 2, a fault is detected at time k when $0 \notin [r_i(k)]$. The information provided by the consistency checking is stored as fault signal $\phi_i(k)$:

$$\phi_i(k) = \begin{cases} 0 \;\; if \;\; 0 \in [r_i(k)] \\ 1 \;\; if \;\; 0 \notin [r_i(k)] \end{cases}. \quad (6)$$

The fault isolation module used in this paper derives from the one proposed in (Puig et al., 2013). The first component is a memory that stores information about the fault signal occurrence history and the fault detection module updates it cyclically (Figure 1).

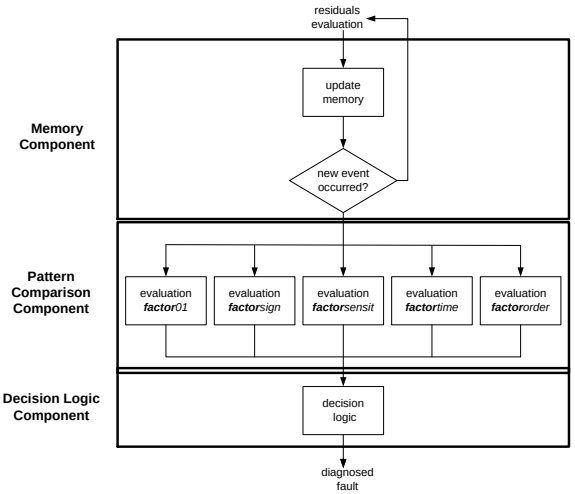

Figure 1. Fault isolation module components

The pattern comparison component compares the memory contents with the stored fault patterns. The standard Boolean fault signature matrix concept (Escobet et al., 2019) is generalized taking into account more fault signal properties (signs, fault sensitivities, etc). The last component represents the decision logic part of the method which aim is to propose the most probable fault candidate.

3.4. Fault prognosis

The detection of fault is forecasted by evaluating the minimum RUL of the set of residual RULs. The RUL_i of each residual is determined as the time for the current k such that $0 \notin [\hat{r}_i(k+RUL_i)]$ according to (5). Every residual has a forecasted fault signal associated at its corresponding RUL: $\hat{\phi}_i(k+RUL_i) = 1$.

The fault prognosis module uses the same logic that the fault isolation algorithms but using the forecasted signals $\hat{\phi}_i(k+RUL_i)$. The forecasted isolation fault at time k can be obtained by analyzing the activated residuals at the end of the corresponding RULs (5).

4. CASE STUDY DESCRIPTION

4.1. BLDC motor model

The constitution of a BLDC motor bears a resemblance to a permanent magnet synchronous machine (PMSM): surface-mounted permanent magnets in the rotor and a 3-phase wye connected winding in the stator. However, its back electro-motive force (emf) induced in the stator is not sinusoidal, as in PMSMs, but trapezoidal (Pillay et al., 1989).

Figure 2(a) (adapted from Xia, 2002) shows the 3-phase equivalent circuit of a BLDC motor powered by a full-bridge inverter, which transforms the DC voltage, V_{dc}, into 3-phase AC voltages, v_{abc}, by means of the switching pattern of 6 Insulated Gate Bipolar Transistors (IGBTs) (S_1,…,S_6) according to the signals given by 3 Hall sensors that detect the rotor position. The following assumptions are made: (a) the stator windings are symmetrical (i.e., they have the same number of turns with same inductance and resistance) and equally distributed in the stator; (b) there is no saturation in the magnetic core; (c) Eddy currents and hysteresis losses are negligible, so there are no iron losses; (d) the armature reaction is ignored; (e) the air-gap magnetic field has a trapezoidal shape, which creates trapezoidal back emfs in the stator windings (as seen in Figure 2(b)); (f) no damper windings are needed in the rotor because permanent magnets have high resistivity; and (g) the permanent magnets are surface-mounted, so there is no saliency, i.e., the airgap thickness is constant; and (h) there is no cogging torque (note that in a salient-pole configuration, slots and teeth are passed by the field magnet and when the rotor moves cogging is generated as a result of reluctance

variation. However, in cylindrical rotors (surface-mounted permanent magnets), there is no reluctance variation (no teeth), so rotation is coggingless (Kenjo et al., 1985)).

According to the previous assumptions, the following differential equations (Pillay et al., 1989) describe the dynamic behavior of a BLDC motor with *p* pole pairs (note that the electrical equations correspond to the equivalent circuit shown in Figure 2(a) and for the mechanical equation the 1-mass model for the shaft has been considered):

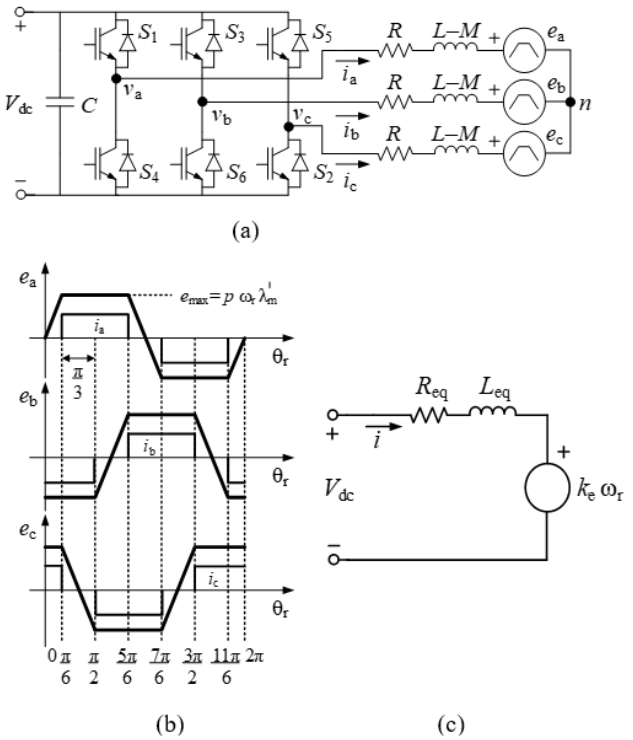

Figure 2. BLDC motor (adapted from Xia, 2002). (a) 3-phase equivalent circuit (motor-sign convention) powered by a full-bridge inverter, (b) trapezoidal per-phase back emfs and per-phase currents in the stator windings, and (c) equivalent circuit under the 2-phase conduction mode (each π/3 rad). Annotation: C = capacitance, e_{abc} = per-phase back emf induced in the stator, i = current of the simplified circuit, i_{abc} = per-phase stator current, k_e = back emf coefficient, L = per-phase self-inductance, L_{eq} = equivalent inductance of the simplified circuit, M = mutual inductance, n = neutral point of the star connection, p = pole pairs, R = per-phase resistance, R_{eq} = equivalent resistance of the simplified circuit, $S_1 \ldots S_6$ = IGBT-based controlled switches, v_{abc} = per-phase stator voltage, V_{dc} = DC voltage, θ_r = rotor angle, λ'_m = amplitude of the flux linkage by the permanent magnets, ω_r = rotor speed.

$$\begin{bmatrix} v_a \\ v_b \\ v_c \end{bmatrix} = \begin{bmatrix} R & 0 & 0 \\ 0 & R & 0 \\ 0 & 0 & R \end{bmatrix} \begin{bmatrix} i_a \\ i_b \\ i_c \end{bmatrix} + \begin{bmatrix} L & M & M \\ M & L & M \\ M & M & L \end{bmatrix} \frac{d}{dt} \begin{bmatrix} i_a \\ i_b \\ i_c \end{bmatrix} + \begin{bmatrix} e_a \\ e_b \\ e_c \end{bmatrix}$$

$$T_e - T_L = J \frac{d\omega_r}{dt} + B_r \omega_r \quad ; \quad T_e = \left(e_a i_a + e_b i_c + e_c i_c \right) / \omega_r \qquad (7)$$

$$\omega_r = \frac{d\theta_r}{dt}$$

where v_{abc} is the per-phase stator voltage, i_{abc} is the per-phase stator current, R is the per-phase resistance, L is the per-phase self-inductance, M is the mutual inductance between each pair of windings, T_e is the electromagnetic torque, T_L is the resisting (or load) torque, J is the moment of inertia of the rotational system (BLDC motor and load), B_r is the damping (or viscous friction) coefficient, ω_r is the rotor speed, θ_r is the rotor angle (whose value is detected by the Hall sensors to obtain the rotor position), d/dt is the differential operator and e_{abc} is the per-phase back emf induced in the stator windings caused by the rotor permanent magnets, whose waveform is shown in Figure 2(b), and whose equation is:

$$\begin{bmatrix} e_a & e_b & e_c \end{bmatrix}^T = p\omega_r \lambda'_m \left[f_a(p\theta_r) \quad f_a(p\theta_r - \frac{2\pi}{3}) \quad f_a(p\theta_r + \frac{2\pi}{3}) \right]^T \qquad (8)$$

where p is the number of pole pairs, λ'_m is the amplitude of the flux linkage established by the permanent magnets in the rotor as viewed from the stator windings, and $f_a(p\theta_r)$ is the trapezoidal function (defined between 1 and –1) shown in Figure 2(b) for phase a. Note that the product $p\theta_r$ corresponds to the electrical angle, θ_e, of the BLDC motor.

It should be noted from the currents i_{abc} shown in Figure 2(b) that there are only 2-phase windings conducting in each interval of π/3 rad (or 60 deg.), which is known as the 2-phase conduction mode of a BLDC motor (Xia, 2002). Let consider that the interval π/3 marked in Figure 2(b), where phases *a* and *b* are conducting and phase *c* is not (switches S_1 and S_6 in Figure 2(a) are turned on and the rest ones are turned off). Under these circumstances, the electrical behavior of the BLDC motor is given by the following equation:

$$\begin{aligned} & v_{ab} = v_{dc} = 2Ri + 2(L - M)\frac{di}{dt} + 2e_a \Rightarrow \\ & \Rightarrow v_{dc} = R_{eq} i + L_{eq} \frac{di}{dt} + k_e \omega_r \end{aligned} \qquad (9)$$

where $i = i_a = -i_b$, $e_a = -e_b$, V_{dc} is the DC bus voltage, $R_{eq} = 2R$ is the equivalent line resistance, $L_{eq} = 2(L - M)$ is the equivalent line inductance, and $k_e = 2p\lambda'_m$ is the coefficient of the back emf. The equivalent circuit that corresponds to (9) is shown in Figure 2(c), which is similar to the equivalent circuit of a series-excited dc motor. The

electromagnetic torque equation given in (7) can now be expressed as:

$$T_e = 2p\lambda_m^{'} i = k_T i \tag{10}$$

where $k_T = 2p\,\lambda_m^{'}$ is the torque coefficient.

Finally, the dynamic behavior of a BLDC motor under the 2-phase conduction mode is given by the electrical equation (9) and by the mechanical equations (the last 2 equations in (7), where the electromagnetic torque is simplified as (10)), giving the following matrix system written in the state-space equation form ($dx/dt = Ax + Bu$, where the state-space variables x are the current, i, and the rotor speed, ω_r):

$$\frac{d}{dt}\begin{bmatrix} i \\ \omega_r \end{bmatrix} = \begin{bmatrix} -\frac{R_{eq}}{L_{eq}} & -\frac{k_e}{L_{eq}} \\ \frac{k_T}{J} & -\frac{B_r}{J} \end{bmatrix}\begin{bmatrix} i \\ \omega_r \end{bmatrix} + \begin{bmatrix} \frac{1}{L_{eq}} & 0 \\ 0 & -\frac{1}{J} \end{bmatrix}\begin{bmatrix} V_{dc} \\ T_L \end{bmatrix} \tag{11}$$

4.2. BLDC motor faults

Brushless DC motors are very reliable devices. However, they can suffer from some failure due to overheating and mechanical wear (Da et al, 2011) and demagnetization (Moosavi et al., 2015). The main faults can generally be categorized in stator faults, rotors faults, inverter faults and bearing faults (Rajagopalan et al., 2006). They can also be classified into electrical faults and mechanical faults. Electrical faults typically involve short-circuited faults of the stator windings and resistive unbalance faults. This kind of fault may produce an unbalance of stator voltages and currents, an increased torque pulsation, a decreased average torque or increased losses and excessive heating.
On the other hand, mechanical faults include eccentricity and bearing faults. They are due to a degradation process in the bearings, destruction of the bearing cage, balls and rollers, and rotor shaft deformation, among others. This kind of fault may result in increased friction for the brushless dc motor. Moreover, necessary sensors for position or current measurement, can fail as well.
In this paper, the following set of faults will be considered:

- faults in sensors: position (f_θ) and current (f_i)
- parametric faults: resistance (f_R), inductance (f_L), friction (f_B) and inertia (f_J)
- systems faults: voltage supply (f_{Vdc}), load (f_{Load})

5. RESULTS

5.1. BLDC motor residuals

Considering the state space model (11), and using the method of generation of structured residuals proposed in (Isermann, 2006), the following residuals can be generated:

$$\begin{aligned} r_1(s) &= R_{eq} I(s) + L_{eq} s I(s) + k_e \omega_r(s) - V_{dc}(s) \\ r_2(s) &= \omega_r(s)(Js + B_r) - k_T I(s) + T_L(s) \\ r_3(s) &= I(s)\left(JL_{eq}s^2 + \left(R_{eq}J + BL_{eq}\right)s + BR_{eq} + k_e k_T\right) - V_{dc}(s)(Js + B) - k_e T_L(s) \\ r_4(s) &= \omega_r(s)\left(JL_{eq}s^2 + \left(R_{eq}J + BL_{eq}\right)s + BR_{eq} + k_e k_T\right) - V_{dc}(s)k_T + \left(L_{eq}s + R_{eq}\right)T_L(s) \end{aligned} \tag{12}$$

These residuals are discretized in time for real-time implementation. Threshold values associated to residuals are computed with maximum absolute values of computed residuals in fault free scenarios.
From the previous four residuals, considering the faults described in Section 4.2, the fault signature matrix (FSM) presented in Table 1 can be obtained.

Table 1. Fault signature matrix

	f_R	f_L	f_{Vdc}	f_B	f_J	f_θ	f_i	f_{Load}
r_1	1	1	1	0	0	1	1	0
r_2	0	0	0	1	1	1	1	1
r_3	1	1	1	1	1	0	1	1
r_4	1	1	1	1	1	1	0	1

5.2. Results of diagnosis

Scenario 1: "Encoder stuck fault"

The position encoder stuck fault scenario consists in losing 20.000 pulses of the encoder (with a resolution of 1024 pulses per revolution) during a small time interval, in this case from 10 to 11 seconds (see Figure 3). As can be seen in the fault signature matrix, the fault affects the residuals r_1, r_2 and r_4 but not r_3. Notice that there is no delay in detecting the fault in residuals r_1, r_2 and r_4 (see Figs 4, 5 and 7).

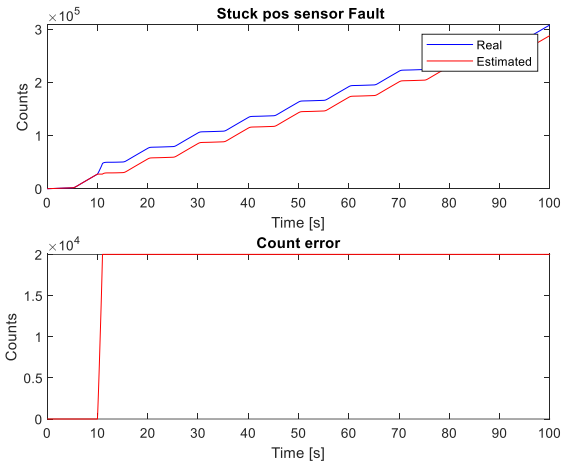

Figure 3. Position sensor fault scenario

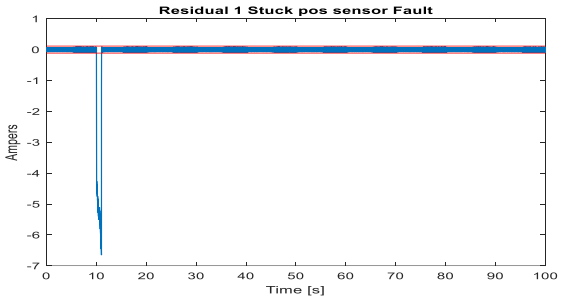

Figure 4. Residual 1 evolution

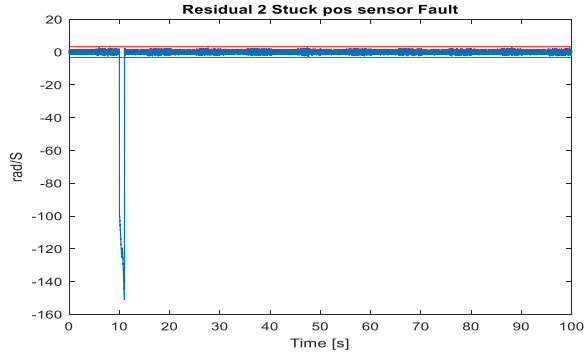

Figure 5. Residual 2 evolution

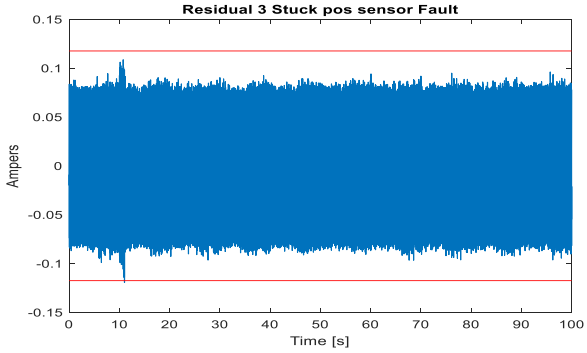

Figure 6. Residual 3 evolution

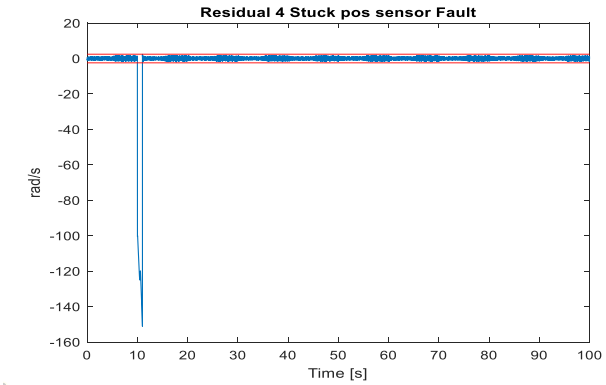

Figure 7. Residual 4 evolution

Analysing the sign of the affected residuals (**factor** *sign* in Figure 1), it can be observed that an encoder stuck situation produces a negative activation of r_1, r_2 and r_4. It can also be seen that these residuals are very sensitive to this fault, because in only one second of encoder pulses loss the motor produces an increase of 4000% of the value of the residual with respect to the threshold (**factor** *sensitivity* in Figure 1). However, this is maintained only during the loss of pulses (stuck situation). Thus, a mechanism of activation holding must be implemented (*memory component* in Figure 1), when the residual overcomes the threshold, to inform about the occurrence of the fault.

5.3. Results of prognosis

Scenario 2: "Incipient leak in the current sensor"

An incipient fault in the current sensor produces a big error until 0.9A after 100 seconds of the simulation scenario. This fault starts at 10 seconds and affects linearly the magnitude of the residuals r_1, r_2 and r_3 but does not affect residual r_4 (see Figs 9, 11, 13 and 14).

All the residuals show a notable level of noise but considering only the mean values of the residuals a delay of approximately 12 seconds can be observed for the activation of the residuals r_1 and r_3 (Figs. 10 and 14) and 15 seconds for r_2 (see Figure 12). In the analysis of the sign of the affected residuals, a positive increase of the big error in the current sensor produces a positive activation of r_1 and r_3 (see Figure 9 and Figure13) and a negative one of r_2 (see Figure 11). Concerning the sensitivity analysis, one can see that the residuals increase in the same manner than the fault (0.9 unities at the end of the scenario) and overcome with a 700% the threshold at the end of the simulated scenario.

This fault produces a constant degradation of the residuals which enables the use of a prognosis method to anticipate the activation time of the residuals, that is the RUL determiner according to (5). The RUL of each residual allows predicting the time to reach its threshold. In this work, the Brown double aliasing technique (4) is very appropriate because firstly the double aliasing reduces

significantly the noise of the residuals and secondly this model allows estimating the Remaining Useful Life (RUL) (5). Figs. 10, 12, 14 and 16 show that the evolution of RUL over time is approaching the real RUL value. These figures show many estimated RUL<0 that become false positive residual activations, which can be easily solved eliminating the estimated RUL below zero. For this scenario, considering an interval of 2% (due to measurement noise), the proposed prognosis method allows to anticipate 9 seconds the activation of r_1, 4 seconds of r2 and around 3.5 seconds of r_3. Consequently, using this prognosis allows anticipating the time for the detection and isolation of this fault as shown in Table 2.

Table 2. Prognosis results

Residual Prognosis	r1	r2	r3	r4
RUL	9 s	4 s	3.5 s	Not affected
Fault detection	Anticipation time of 9 seconds to the real fault detection			
Fault isolation	Anticipation time of 3.5 seconds to the real fault isolation			

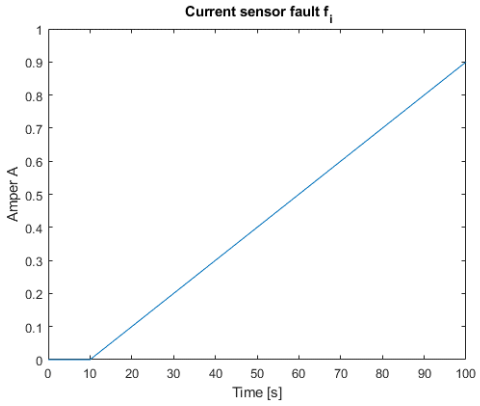

Figure 8. Current sensor fault

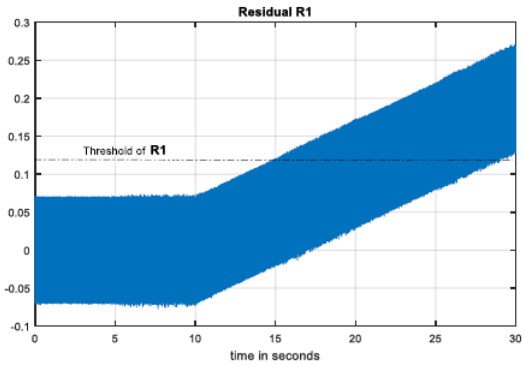

Figure 9. Evolution of r_1 current fault

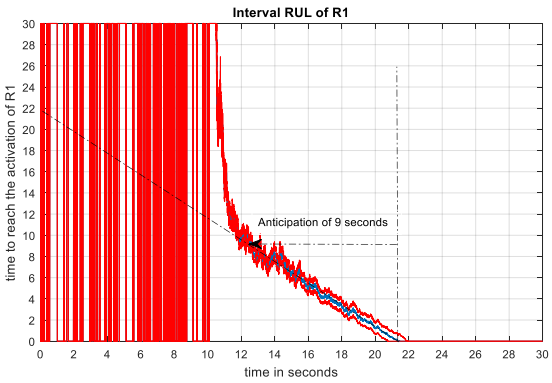

Figure 10. RUL of r_1

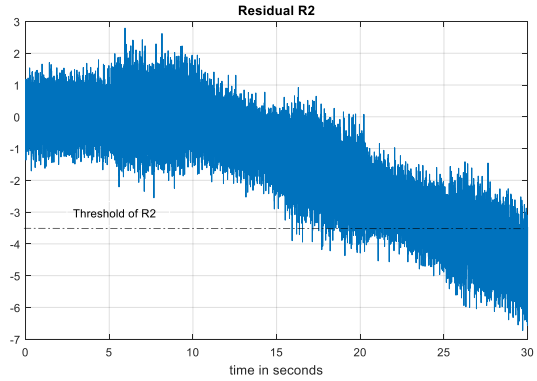

Figure 11. Evolution of r_2 current fault

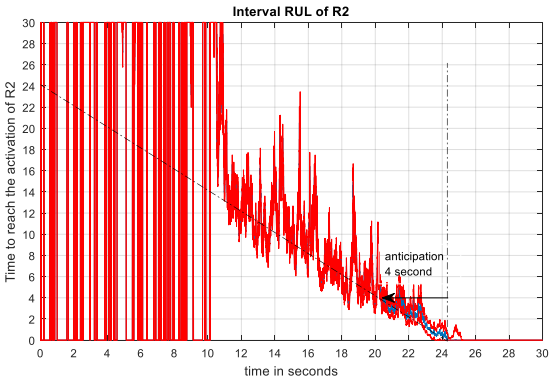

Figure 12. RUL of r_2

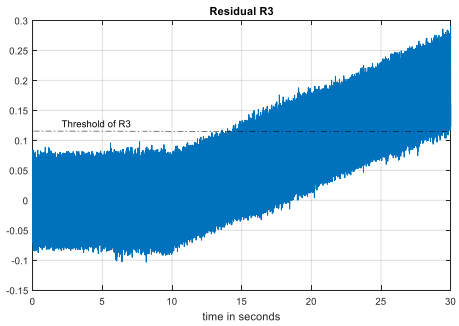

Figure 13. Evolution of r_3 current fault

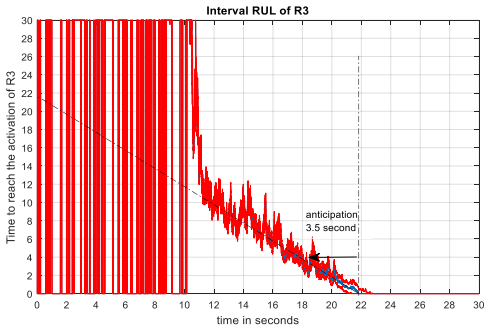

Figure 14. RUL of r_3

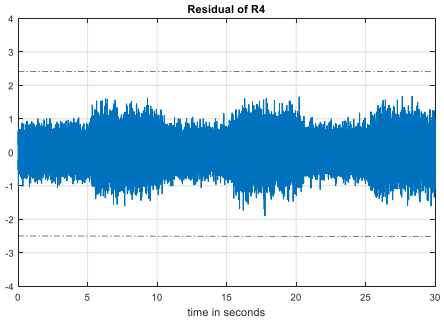

Figure 15. Evolution of r_4 current fault

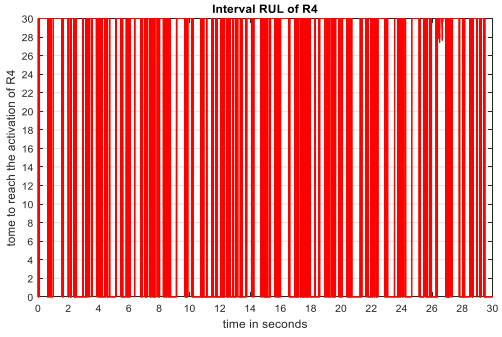

Figure 16. RUL of r_4

6. CONCLUSIONS

This paper has proposed a model-based fault diagnosis and prognosis approach for brushless DC motors (BLDC). A simplified model extracted from the BLDC motor equations has been used to generate four structural residuals. The on-line evaluation of the inconsistency of computed residuals allows the fault diagnosis (detection and isolation) of the considered mechanical and electrical faults. Inconsistency of a residual is determined if its absolute value is above a threshold computed from non-faulty data. A Double Exponential Smoothing filter is applied to residuals in order to predict future inconsistencies of residuals a therefore future faults. The proposed model-based is an alternative to vibration-based diagnostics because residuals are computed from analytical redundancy relations between measured and estimated variables that are already available in BLDC motors for control purposes. A realistic simulator has been used to evaluate the performance of the proposed method obtaining satisfactory results in both fault diagnosis and prognosis for the different fault scenarios.

ACKNOWLEDGEMENT

This work has been funded by the Spanish State Research Agency (AEI) and the European Regional Development Fund (ERFD) through the project SCAV (ref. MINECO DPI2017-88403-R), by the DGR of Generalitat de Catalunya (SAC group ref. 2017/SGR/482) and by SMART Project (ref. num. EFA153/16 Interreg Cooperation Program POCTEFA 2014-2020). Joaquim Blesa and Alejandro Rolán acknowledge the support from the Serra Húnter program.

REFERENCES

Blanke, M., Kinnaert, M., Lunze, J., Staroswiecki, M. (2006) Diagnosis and Fault-Tolerant Control. Springer, 2nd edition.

Da, Y., Shi, X., Krishnamurthy, M. (2011) Health monitoring, fault diagnosis and failure prognosis techniques for brushless permanent magnet machines. In 2011 IEEE Vehicle Power and Propulsion Conference, Chicago, IL, pp. 1–7.

Ding, S. X. (2008) Model-based Fault Diagnosis Techniques. Springer.

Escobet, T., Bregon, A., Pulido, B., Puig, V. (2019) Fault Diagnosis of Dynamic Systems. Springer.

Isermann, R. (2006) Fault-diagnosis systems: an introduction from fault detection to fault tolerance. Springer.

Kenjo, T., Nagamori, S. (1985) Permanent-magnet and brushless DC motors. Oxford University Press.

Moosavi, S.S., A. Djerdir, Y. Ait. Amirat, D.A. Khaburi, (2015) Demagnetization fault diagnosis in permanent magnet synchronous motors: A review of the state-of-

the-art. Journal of Magnetism and Magnetic Materials, 391, pp.203–212.

Pillay, P., Krishnan, R. (1989) "Modeling, simulation, and analysis of permanent-magnet motor drives. Part II: the brushless dc motor drive," IEEE Trans. Ind. App., vol. 25, no. 2, pp. 274-279.

Puig, V., Blesa, J. (2013) "Limnimeter and rain gauge FDI in sewer networks using an interval parity equations based detection approach and an enhanced isolation scheme", Control Engineering Practice, Volume 21, Issue 2, Pages 146-170.

Rajagopalan, S., Aller, J. M., Restrepo, J. A., Habetler, T. G., Harley, R. G. (2006) "Detection of Rotor Faults in Brushless DC Motors Operating Under Nonstationary Conditions". IEEE Trans. Ind. App., vol. 42, no. 6, pp. 1464-1477.

Roychoudhury, I., Biswas, G., Koutsoukos, X. (2006). "A Bayesian Approach to Efficient Diagnosis of Incipient Faults," in Prod. 17th international Workshop on Principles of Diagnosis, Peñaranda de Duero, Spain.

S. Hansun, A new approach of Brown's double exponential smoothing method in time series analysis, Balkan Journal of Electrical and Computer Engineering 4 (2016) pp.75-78.

Xia, C. L. (2002). Permanent Magnet Brushless DC Motor Drives and Controls. Wiley.

Yu, M., Wang, D., Luo, M., Huang, L. (2011). "Prognosis of Hybrid Systems with Multiple Incipient Faults: Augmented Global Analytical Redundancy Relations Approach," IEEE Trans. Syst., Man, and Cybern - part A: Syst. and Hum., vol. 42, no. 3, pp. 1083-4427.